NACA0012 AIRFOIL LABORATORY REPORT – COURSEWORK 1

Name: Ioana Ispas

Student ID: 210061590

Module code: EMS514U

Module Title: Subsonic Aerodynamics and Wings

Coursework Name: Pressure Distribution and Lift on a NACA0012 Aerofoil

Raw Data: Group 02B

Apparatus and Instrumentation

The apparatus in this experiment consisted of a symmetrical constant chord wing with its uniform cross-section positioned vertically in a low-speed open return wind tunnel, where its angle of incidence is varied at 3-degree intervals from 3° to 12°. The wing consisted of built-in tubes at the leading and trailing edge tappings, as well as 28 tubes placed at equal intervals across the upper and lower tappings of the model, all linked to an inclined multi-tube manometer containing methylated spirit. A pitot-static tube was used to measure the static and stagnation pressure at the beginning of the experiment. A mercury barometer and mercury thermometer were used to measure the atmospheric pressure and temperature respectively.

Raw Data

Table 1: Raw data acquired from Manometer Readings

Tapping	i=3 (cm)	i=6 (cm)	i=9 (cm)	i=12 (cm)
1	16.60	21.40	27.40	20.80
2	26.80	30.40	37.20	27.00
3	17.00	16.60	16.00	16.00
4	25.60	28.60	29.80	27.00
5	20.80	19.60	18.40	18.20
6	26.00	27.20	28.00	26.60
7	21.40	20.00	19.20	19.20
8	25.00	26.20	27.00	26.60
9	21.80	20.80	17.80	20.00
10	24.20	25.40	26.20	26.60
11	22.00	20.80	21.00	20.00
12	24.20	24.20	25.80	26.40
13	22.00	20.80	20.20	20.20
14	24.00	24.60	25.00	26.20
15	21.80	21.00	20.60	20.40
16	23.80	24.20	24.80	26.00
17	21.80	21.00	20.60	20.80
18	20.40	20.80	21.20	22.40
19	21.80	21.20	20.80	20.60
20	23.20	21.60	23.80	25.20
21	21.80	21.20	20.80	21.00
22	22.80	23.00	23.00	24.20
23	21.60	21.20	21.00	21.00
24	22.40	22.60	22.60	24.00
25	21.40	21.20	21.00	21.20
26	22.00	22.20	22.00	24.00
27	21.20	21.20	21.20	20.60
28	21.40	21.60	21.40	23.40
29	21.00	21.00	21.20	22.00
30	20.80	20.80	21.20	22.60

Table 2: Raw Background Data

Atmospheric Pressure/H (mbar)	Atmospheric Temperature/ T (°C)	Manometer inclination angle/β (°)	Density of Manometer (kg/m3)
1020	20.6	45	813.86
Density of mercury/ρH G (kg/m3)	**Gravitational constant/g (m/s2)**	**Specific Gas Constant/ Rspecific (m2s-2K-1)**	**Sutherland's Constant/S (K)**
13.6*10^3	9.807	287.3	110.4
Stagnation Pressure/lt (cm of meth. spirit)	**Static Pressure/ls (cm of meth. spirit)**	**Stagnation-static/Δl (cm of meth. spirit)**	
15.8	21	5.2	
Reference Viscosity/μref (kgm-1s-1)	**Reference Temperature/ Tref (K)**	**Chord Length/c (mm)**	
1.789*10^-5	288.2	150	

Sample Calculations

1. Ambient air pressure:

$$p_{at} = H_{at} * 100 = 1020 * 100 = 102000Pa$$

2. Absolute temperature:

$$T_{at} = t_{at} + 273.16K = 293.76K$$

3. Density for air in wind tunnel:

$$\rho_{air} = \frac{P_{at}}{RT_{at}} = \frac{102000}{287.3 * 293.76} = 1.20857\ kg/m^3$$

4. Viscosity of air in wind tunnel:

$$\mu_{air} = \mu_{ref} * \left(\frac{T_{ref} + S}{T_{at} + S}\right) * \left(\frac{T_{at}}{T_{ref}}\right)^{\frac{3}{2}} = 1.789 * 10^{-5} * \left(\frac{288.2 + 110.4}{293.76 + 110.4}\right) * \left(\frac{293.76}{288.2}\right)^{\frac{3}{2}} = 1.81569 * 10^{-5} kgm^{-1}s^{-1}$$

5. Difference in static and total pressure:

$$(p_t - p_s) = \rho_{MS} * g * \Delta h * sin\beta = 813.86 * 9.807 * 0.052 * sin45 = 293.4771Pa$$

6. Tunnel speed:

$$V_\infty = \sqrt{\frac{2 * (p_t - p_s)}{\rho}} = \sqrt{\frac{2 * 293.4771}{1.20857}} = 22.03769\ m/s$$

7. Chordal Reynolds Number:

$$Re_c = \frac{\rho_{air} V_\infty c}{\mu} = \frac{1.20857 * 22.03769 * 0.15}{1.81569 * 10^{-5}} = 220032.894$$

8. Pressure Coefficient (Cp) for tapping number 3 at i=3:

$$C_{p3} = \frac{(l_n - l_s)}{(l_t - l_s)} = \frac{(17 - 21)}{(15.8 - 21)} = 0.7692$$

9. ΔCp at i=3 at x/c = 0.05:

$$\Delta C_p = \left(C_{pl} - C_{pu}\right) = (0.7692 - (-1.1154)) = 1.8846$$

10. Theoretical value of ΔCp at i=3 when x/c = 0.1:

$$\Delta C_p = 4\alpha \sqrt{\frac{1 - \bar{x}}{\bar{x}}} = 4 * 0.05236 \sqrt{\frac{1 - 0.1}{0.1}} = 0.6283$$

11. Lift Coefficient C_L for i=3:

$$C_L = C'_L \cos\alpha = \cos(0.05236) * \int_0^1 C_{Pls} - C_{Pus}\, d\left(\frac{x}{c}\right) = 0.3697$$

12. Lift curve slope value calculated between α=3 and α=9 (in radians):

$$\frac{dC_L}{d\alpha} = \frac{C_{Li=9} - C_{Li=3}}{\alpha_{i=9} - \alpha_{i=3}} = \frac{0.8087 - 0.3702}{0.1571 - 0.05326} = 4.09677$$

Processed Data

Table 3: Processed data displaying negative pressure coefficient values for all angles of incidence

	i=3		i=6		i=9		i=12	
x/c	Upper -Cp i=3	Lower -Cp i=3	Upper -Cp i=6	Lower -Cp i=6	Upper -Cp i=9	Lower -Cp i=9	Upper -Cp i=12	Lower -Cp i=12
0	-0.8462	-0.8462	-1.0769	-1.0769	1.2308	1.2308	-0.0385	-0.0385
0.05	1.1154	-0.7692	1.8077	-0.8462	3.1154	-0.9615	1.1538	-0.9615
0.1	0.8846	-0.0385	1.4615	-0.2692	1.6923	-0.5000	1.1538	-0.5385
0.15	0.9615	0.0769	1.1923	-0.1923	1.3462	-0.3462	1.0769	-0.3462
0.2	0.7692	0.1538	1.0000	-0.0385	1.1538	-0.6154	1.0769	-0.1923
0.25	0.6154	0.1923	0.8462	-0.0385	1.0000	0.0000	1.0769	-0.1923
0.3	0.6154	0.1923	0.6154	-0.0385	0.9231	-0.1538	1.0385	-0.1538
0.35	0.5769	0.1538	0.6923	0.0000	0.7692	-0.0769	1.0000	-0.1154
0.4	0.5385	0.1538	0.6154	0.0000	0.7308	-0.0769	0.9615	-0.0385
0.45	-0.1154	0.1538	-0.0385	0.0385	0.0385	-0.0385	0.2692	-0.0769
0.5	0.4231	0.1538	0.1154	0.0385	0.5385	-0.0385	0.8077	0.0000
0.6	0.3462	0.1154	0.3846	0.0385	0.3846	0.0000	0.6154	0.0000
0.7	0.2692	0.0769	0.3077	0.0385	0.3077	0.0000	0.5769	0.0385
0.8	0.1923	0.0385	0.2308	0.0385	0.1923	0.0385	0.5769	-0.0769
0.9	0.0769	0.0000	0.1154	0.0000	0.0769	0.0385	0.4615	0.1923
1	-0.0385	-0.0385	-0.0385	-0.0385	0.0385	0.0385	0.3077	0.3077

Table 4: Data displaying processed and theoretical Delta Pressure coefficient values for all angles of incidence

		Processed data for ΔCp				Theoretical data for ΔCp			
Tapping numbers (upper/lower)	x/c	i=3	i=6	i=9	i=12	i=3	i=6	i=9	i=12
1	0	0.000	0.000	0.000	0.000	0.000	0.000	0.000	0.000
2/3	0.05	1.8846	2.6538	4.0769	2.1154	0.9129	1.8259	2.7388	3.6517
4/5	0.1	0.9231	1.7308	2.1923	1.6923	0.6283	1.2566	1.8850	2.5133
6/7	0.15	0.8846	1.3846	1.6923	1.4231	0.4986	0.9971	1.4957	1.9943
8/9	0.2	0.6154	1.0385	1.7692	1.2692	0.4189	0.8378	1.2566	1.6755
10/11	0.25	0.4231	0.8846	1.0000	1.2692	0.3628	0.7255	1.0883	1.4510
12/13	0.3	0.4231	0.6538	1.0769	1.1923	0.3199	0.6398	0.9598	1.2797
14/15	0.35	0.4231	0.6923	0.8462	1.1154	0.2854	0.5708	0.8563	1.1417
16/17	0.4	0.3846	0.6154	0.8077	1.0000	0.2565	0.5130	0.7695	1.0260
18/19	0.45	-0.2692	-0.0769	0.0769	0.3462	0.2315	0.4631	0.6946	0.9262
20/21	0.5	0.2692	0.0769	0.5769	0.8077	0.2094	0.4189	0.6283	0.8378
22/23	0.6	0.2308	0.3462	0.3846	0.6154	0.1710	0.3420	0.5130	0.6840
24/25	0.7	0.1923	0.2692	0.3077	0.5385	0.1371	0.2742	0.4113	0.5484
26/27	0.8	0.1538	0.1923	0.1538	0.6538	0.1047	0.2094	0.3142	0.4189
28/29	0.9	0.0769	0.1154	0.0385	0.2692	0.0698	0.1396	0.2094	0.2793
30	1	0.000	0.000	0.000	0.000	0.000	0.000	0.000	0.000

Table 5: Lift coefficient data

α	C'L	Uncertainty	CL	Uncertainty
3	0.3702	±0.00003	0.3697	±0.007
6	0.5769	±0.00005	0.5738	±0.003
9	0.8087	±0.00002	0.7987	±0.002
12	0.8394	±0.00002	0.8211	±0.004

Table 6: Processed data values

Ambient Air Pressure/pat (Pa)	Absolute Temperature/ Tat (K)	Density of air in wind tunnel/ρ (kg/m^3)	Viscosity of air in wind tunnel/μ (kgm^-1s^-1)
1.02*10^5	293.76	1.20857	1.81569*10^-5
Tunnel speed/V∞ (m/s)	**Chordal Reynolds number/Rec**	**Lift curve slope/ dCl/dx**	
22.03769	2.2*10^5	4.09677	

Results

Figure 1: Graph displaying the negative pressure coefficient v against x/c profile along a NACA0012 aerofoil

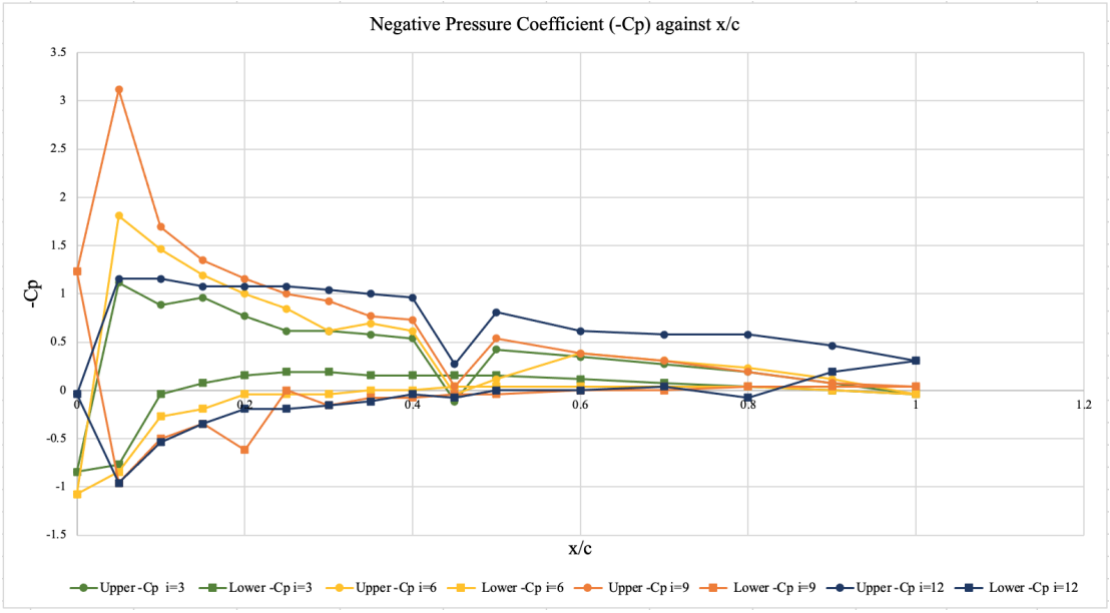

Figure 2: Graph displaying experimental and theoretical values for delta pressure coefficient against x/c for all 4 angles of incidence of a NACA0012 aerofoil

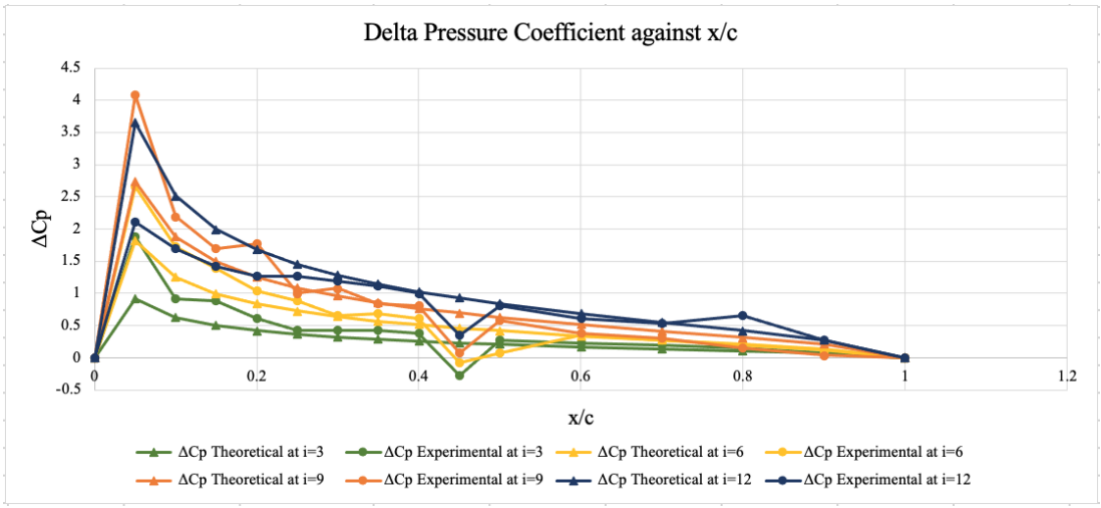

Figure 3: Graph displaying Coefficient of lift against α (°) for all angles of incidence

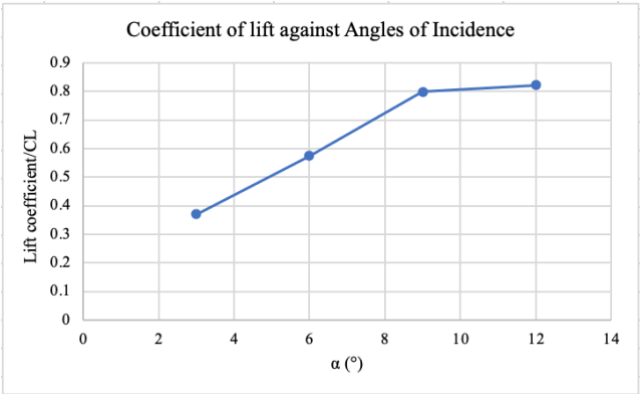

Discussion

Learning Outcome:

The learning outcome of this experiment was to examine the changes in pressure as the angle of incidence on a NACA0012 airfoil is increased, and to identify when stall occurs based on the changes in pressure and lift coefficient results.

Difficulties encountered:

As the angle of incidence was increased at around 9° and above, the spirit levels in the manometer fluctuated significantly, making it difficult to procure an accurate value for each tapping. This had the potential to cause human errors in the data. Furthermore, tapping 18 on the air foil was not connected correctly to the manometer, thus causing evident discrepancies in the collected data.

General Trends:

As the angle of incidence is increased, instability is experienced in the upper section closer to the leading edge and in the lower section closer to the trailing edge [Schlichting, 1979]. This can be seen in Figure 1, where the negative pressure coefficient for the upper side of the aerofoil peaks closer to the leading edge at 9° incidence and has a positive pressure coefficient value at the trailing edge, suggesting that the aerofoil is reaching its stall angle, further characterised by the sudden drop in lift between 9° and 12° seen in Figure 3, where the line begins to plateau after an angle of attack of 9°. It also adheres to the theoretical response, as when the pressure gradient is too adverse due to the angle of attack being too large, the boundary layer will separate from the surface [Gerhart et al., 2017]. According to theory, as the angle of attack of an aerofoil is increased, the pressure difference between the maximum point of the aerofoil and the trailing edge increases and the separation point moves forward [Barnard & Philpott, 1994]. When calculating lift coefficient, the straight-line approximation could have also been used.

As evident in Figure 2, the pressure difference is greatest roughly where the maximum point on the aerofoil is found, further promoting the theory behind the pressure distribution. At the leading edge for angles 6°,9° and 12°, the delta pressure coefficient is significantly greater than that of the theoretical ΔCp values, signifying possible errors or anomalies in the data caused by the manometer spirit level fluctuations. However, the pressure values start adhering to the theoretical closer to the trailing edge, adopting the theoretical line. The use of the Bernoulli equation provided the equation used for finding the pressure coefficient values, however, this could have also been achieved with Euler's equation, which would have required the use of the streamlines around the aerofoil to calculate the pressure around the wing shape [Nakamura].

The lift slope value for this experiment is 4.09677 as shown in Table 6, whilst the common value is around 6.2832 for a NACA0012 aerofoil [Anderson, 2017], which suggests that there were discrepancies in the data such as tapping 18 that may have skewed the data produced.

Possible improvements:

As a future improvement, taking multiple readings for each tapping would be the most suitable method to eliminate error from fluctuating spirit levels. Using the exact freestream pressure instead of the static pressure would produce more accurate pressure coefficient values by connecting tappings to a Betz manometer. Increasing the number of angles of incidences experimented would be beneficial, in order to find the exact angle of stall more accurately.

Errors and Uncertainty calculations:

CL uncertainty: $\delta f(x,y) = \sqrt{\left(\frac{\partial f}{\partial x} \times \delta x\right)^2 + \left(\frac{\partial f}{\partial y} \times \delta y\right)^2} = \pm 0.005$

Conclusion:

Overall, this experiment showed that as the angle of incidence increases on a symmetrical aerofoil, the boundary layer begins to separate due to the increase in adverse pressure experienced from the maximum point to the trailing edge of the aerofoil. Despite the difficulties in obtaining data due to faulty equipment, the overall trend of the calculated values mostly adheres to the theoretical concepts and data compared to, thus concluding that this experiment was a success.

References

Anderson, J.D. (2017) *Fundamentals of aerodynamics*. New York: McGraw-Hill Education.

Barnard, R.H. and Philpott, D.R. (1994) *Aircraft flight: A description of the physical principles of Aircraft Flight*. Prentice Hall.

Gerhart, P.M., Gerhart, A.L. and Hochstein, J.I. (2017) "Flow over Immersed Bodies", in *Munson's Fluid Mechanics*. Hoboken (NJ): Wiley.

Nakamura, M. (no date) *2.972 how an airfoil works*. Available at: https://web.mit.edu/2.972/www/reports/airfoil/airfoil.html (Accessed: February 17, 2023).

Schlichting, H. (1979) *Boundary-layer theory*. New York: McGraw-Hill.